Chemical Science International Journal

Volume 33, Issue 1, Page 22-35, 2024; Article no.CSIJ.111342
ISSN: 2456-706X
(Past name: American Chemical Science Journal, Past ISSN: 2249-0205)

Synthesis, Characterization, Fluorescence and Antibacterial Activities Studies of Transition Metals Complexes with a Macro Acyclic Schiff Base Ligand

Fatou Barr [a], Ndèye Fatou Ndiaye [a], Antoine Blaise Kama [a], Farba Bouyagui Tamboura [a*], Moussa Dieng [a], Rianatou Bada Alambedji [b], Ibrahima Elhadji Thiam [c], Aliou Hamady Barry [d], Nicolas Claiser [e], Mohamed Souhassou [e] and Mohamed Lamine Gaye [c]

[a] Department of Chemistry, UFR SATIC, University Alioune DIOP, Bambey 21400, Senegal.
[b] Laboratory of Microbiology, Immunology and Infectious Pathology of Dakar, Senegal.
[c] Department of Chemistry, University Cheikh Anta Diop, Dakar 10700, Senegal.
[d] Unité de Recherche en Chimie des Matériaux, Department of Chemistry, Faculty of Sciences and Technics, University of Nouakchott, Mauritania.
[e] Laboratory CRM2, UMR CNRS 7036, Institut Jean Barriol, University of Lorraine, 54506, Vandœuvre-lès-Nancy, France.

Authors' contributions

This work was carried out in collaboration among all authors. All authors read and approved the final manuscript.

Article Information

DOI: 10.9734/CSJI/2024/v33i1882

Open Peer Review History:
This journal follows the Advanced Open Peer Review policy. Identity of the Reviewers, Editor(s) and additional Reviewers, peer review comments, different versions of the manuscript, comments of the editors, etc are available here: https://www.sdiarticle5.com/review-history/111342

Original Research Article

Received: 26/10/2023
Accepted: 30/12/2023
Published: 08/01/2024

**Corresponding author: E-mail: farba.tamboura@uadb.edu.sn;*

ABSTRACT

The reactions of the Schiff base 2,2'-[(2-hydroxypropane-1,3-diyl) bis-(imino-methane diyl)] bis-(4-bromophenol) (H3L), with metal transition ions (Mn(II), Ni(II), Cu(II), Zn(II), and Cd(II),) afforded one type of complex formulated as [M(HL)(H2O)2].nH2O. These compounds have been characterized by elemental analysis, UV–Vis, FTIR, 1H and 13C NMR spectroscopies, molar conductivity and room temperature magnetic measurements. The structure of nickel (II) complex has been determined by X-ray crystallography. The complex crystallizes in the orthorhombic space group Pnma with a = 7.7702(4) Å, b = 23.1921(15) Å, c = 10.6853(5) Å, V = 1925.57(15) Å3, Z = 8, R1 = 0.043 and wR2 = 0.107, Dcalc = 1.893 Mg m−3. The ligand acts in tetradentate fashion in its di-deprotonated form. Two coordinated water molecules complete the coordination sphere. The environment around the Ni(II) center is best described as an octahedral geometry. In the crystal structure of the Schiff base ligand, the existence of a strong intramolecular O-H•••O hydrogen bonding [O2W-H2W 0.80(3) Å, H2W •••O1 1.915(3) Å, O2W••• O1 2.6258(19) Å, O2W-H2W•••O1 148(3)°] and [O1W-H1W 0.73(3), H1W•••O1 2.15(4) Å, O1W•••O1 2.836(2)Å, O1W-H1W•••O1 156(4)°] are observed. Antibacterial activity study shows that the cadmium (II) complex is more active than the free ligand on.

Keywords: Schiff base; antibacterial activity; metal complex; FTIR; magnetic; X-ray diffraction.

1. INTRODUCTION

"Schiff bases obtained by condensation of nicotinic hydrazide and a ketoprecursor are widely used in the synthesis of transition metal complexes" [1-3]. Those complexes are particularly interesting in various fields such as magnetism [4,5], catalysis [6], medicine [7] and antibacterial activities are also reported [8,9]. "In recent studies, nicotinic hydrazide complexes have been prepared and have shown enzyme-like activities" [10,11]. "In the present paper, we report the synthesis and the structural characterization of transition metal complexes with the hydrazone ligand H_3L (2,2'-[(2-hydroxypropane-1,3-diyl)bis(imino-methanediyl)]bis(4-bromophenol)). The powder compounds were characterized with spectroscopic techniques. The new Nickel(II) complex formulated as $[Ni(HL)(H_2O)_2]$ was characterized with X-ray diffraction" [10,11]. The study of the behaviour of transition metals (3d) incorporated in ligands is of particular interest to chemists. Mono and polynuclear complexes of transition metals have been the subject of several studies. The physical and chemical properties of complexes are determined both by their geometry and by the nature of the electron density around the metal. Recently, we have been focusing on the synthesis of ligands and their complexes for biological applications such as antioxidant [12], antibacterial [13] and antimicrobial activities [14,15]. The present work involves the synthesis of a di-azomethine ligand by condensation reaction between a diamine and a ketoprecursor. Based on di-azomethine ligands, transition metal complexes are synthesized and characterized by physical and chemical analysis methods, and some are used in biological assays to determine possible activities.

2. EXPERIMENTAL

2.1 Materials and Procedures

5-Bromo-benzaldehyde, diamino-1,3-propan-2-ol as well as $M(X)_2{\cdot}nH_2O$ (M = Mn(II), Ni(II), Cu(II), Cd(II) and X = NO_3, OAc) were commercial products (from Alfa and Aldrich) and were used without further purification. Solvents were of reagent grade and were purified by the usual methods. Elemental analyses were performed in a Carlo-Erba EA microanalyser. Infrared spectra were recorded as KBr discs on a Bruker IFS-66V spectrophotometer. LSI-MS were recorded using a Micromass Autospec spectrometer with 3-nitrobenzyl alcohol as the matrix. The ^{1}H and ^{13}C NMR spectra were recorded in DMSO-d_6 on a BRUKER 500 MHz spectrometer at room temperature using TMS as an internal reference. The UV-Vis spectra were run on a Shimadzu UV-2501 PC Recording spectrophotometer (1000 – 200 nm). The molar conductance of 10^{-3} M in DMF solutions of the metal complexes was measured at 25 °C using a WTW LF-330 conductivity meter with a WTW conductivity cell. Room temperature magnetic susceptibilities of the powdered samples were measured using a Johnson Mattey scientific magnetic susceptibility

balance {calibrant $Hg[Co(SCN)_4]$}. Melting points were recorded on a Büchi apparatus and are uncorrected.

2.1.1 Evaluation of the antibacterial activity of schiff bases

Basic microbiological equipment: These are small items of equipment used to perform microbiological tests, such as petri dishes, platinum loop, proline micropipette, graduated cylinder, tubes, vortex mixer, densitometer, blank 6 mm diameter discs not soaked in antibiotics and 96-well plates for MIC. For a large-scale equipment, such as an electronic balance, an oven set at 37°C, an autoclave at 120°C, a plate-type shaker, a magnifying glass or MIC reading device, and a refrigerator for storing samples. Consumables include gloves, sterile physiological water and DMSO. Culture media are Muller Hinton Agar (MH): These are small items of equipment used to perform microbiological tests, such as petri dishes, platinum loop, proline micropipette, graduated cylinder, tubes, vortex mixer, densitometer, blank 6 mm diameter discs not soaked in antibiotics and 96-well plates for MIC. For large-scale equipment, such as an electronic balance, an oven set at 37°C, an autoclave at 120°C, a plate-type shaker, a magnifying glass or MIC reading device, and a refrigerator for storing samples. Consumables include gloves, sterile physiological water and DMSO. Culture media are Muller Hinton Agar (MH).

Assessment of antibacterial activity: The antibacterial activity of the products synthesized was evaluated on three bacterial strains: Escherichia coli, Salmonella. SP and Pasteurella multocida. This evaluation is carried out in the Microbiology, Immunology and Infectious Pathology Laboratory (MIPI). The method used is that of disc diffusion on Muller-Hinton agar, taking into account the recommendations of the Antibiogram Committee of the French Microbiology Society (EUCAST/CA-SFM, 2013). The solvent used is DMSO. These recommendations concern the preparation of the Muller-Hinton culture medium, the bacterial inoculum, and the choice and arrangement of disks.

Determining MICs: It is necessary to start with sensitivity testing before determining the MIC. The MIC is the Minimum Inhibitory Concentration, defined by the EUCAST (European Society of Clinical Microbiology and Infectious Disease) committee as the lowest concentration of compound capable of inhibiting the growth of microorganisms in a given period of time. To determine MICs, we use double dilution plates to determine the lowest concentration for each sample at which the strains are sensitive. Concentrations ranging from 15 to 0.029 mg/mL are determined using the standard MIC technique.

2.2 Synthesis of the H_3l Ligand and its Transition Metal Complexes

2.2.1 Synthesis of ligand 2,2'-[(2-hydroxypropane-1,3-diyl) bis (imino-methane diyl)] bis (4-bromophenol): H_3L

In a 250 mL flask containing 20 mL of ethanol, 0.897 g (10 mmol) of 1,3-diaminopropan-2-ol was added. A solution of 4 g (20 mmol) of 5-bromo-salicylaldehyde, dissolved in 50 mL of ethanol was added. The mixture was stirred and refluxed for two hours to yield a yellow precipitate. On cooling, the resulting suspension was filtered. The yellow solid was washed with 2 x 10 mL of ether and air-dried. Yield: 89%. Melting point: 140°C. Calculated for $C_{17}H_{16}Br_2N_2O_3$, C, 44.76; H, 3.54; N, 6.14. Found C, 44.78; H, 3.56; N, 6.07. IR (ν, cm^{-1}) 3113, 2863, 1650, 1620, 1569, 1508, 1471, 1400, 1371, 1346, 1332, 1292, 1270, 1240, 1206, 1183, 1161, 1129, 1101, 1074, 1041, 998, 977, 894, 862, 821, 779, 698, 674, 628, 617, 576, 557, 538, 511, 465. NMR ^1H (300 MHz, DMSO-d_6, δ (ppm)): 3.36 (d, 4H, $–H_2C–$); 3.65 (m, 1H, HC); 5.24 (s, 1H, HO–CH); 6.8 (s, 2H, H_{Ar}); 7.4 (d, 2H, H_{Ar}); 7.67 (s, 2H, H_{Ar}); 8.51 (s, 2H, HC=N); 13.65 (s, 2H, HO–Ar). RMN ^{13}C, (300 MHz, DMSO-d_6, δ (ppm)): 62.38 ($–H_2C–$); 69.02 (HO–CH); 108.78 (C_{Ar}); 119.11 (C_{Ar}); 120 (C_{Ar}); 133.43 (C_{Ar}); 134.72 (C_{Ar}); 160.49 (C=N); 165.84 (HO–C_{Ar}). UV-Vis (λ, nm): 265, 280, 331, 362.

2.2.2 Synthesis of transition metal complexes from the H_3L ligand

2.2.2.1 Complexes from metal chloride salts

(0.2 g, 0.435 mmol) of H_3L was dissolved in 10 mL of absolute ethanol. A solution of $MCl_2{\cdot}xH_2O$ (M = Mn, Ni, Zn and Cd) (0.435 mmol) in 10 mL of absolute ethanol. The two solutions were mixed, and the resulting solution was then refluxed for two hours. After cooling, the solution was filtered and slowly evaporated. Only the complex from cadmium chloride precipitate.

$[Mn(HL)(H_2O)_2]\cdot H_2O$ (1), IR (ν, cm^{-1}): 3223, 1612, 1463, 1426, 1372, 1271, 1204, 1172, 1152, 892, 827, 766, 705, 685. Λ ($\Omega^{-1}\cdot cm^2\cdot mol^{-1}$) : 23 and 26 two weeks after. MP (°C) = 220. μeff: 5.54 μB. Uv-vis (DMF, λ_{max}, nm): 395, 412, 430, 472, 515, 576, 583. Calculated for $C_{17}H_{20}Br_2N_2O_6Mn$ (%): C, 36.26; H, 3.58; N, 4.97. Found (%): C, 36.42; H, 3.63; N, 4.87.

$[Ni(HL)(H_2O)_2]$ (2), IR (ν, cm^{-1}): 3671, 3319, 2901, 1625, 1532, 1467, 1395, 1305, 1249, 1176, 1137, 1077, 1052, 968, 828, 803. μeff: 2.68 μB. UV-Vis (DMF, λ_{max}, nm): 282, 371, 428, 606. Λ ($\Omega^{-1}\cdot cm^2\cdot mol^{-1}$) : 27 and 32 two weeks later. Yield: 85%. MP(°C) > 260. Calculated for $C_{17}H_{18}Br_2N_2O_5Ni$ (%): C, 37.20; H, 3.31; N, 5.10. Found (%): C, 37.34; H, 3.43; N, 5.02.

$[Zn(HL)(H_2O)_2]\cdot H_2O$ (3), IR (ν, cm^{-1}): 3111, 2231, 1593, 1571, 1501, 1433, 1323, 1290, 1263, 1176, 1159, 1014, 831. Λ ($\Omega^{-1}\cdot cm^2\cdot mol^{-1}$) : 25 and 28 two weeks after. MP(°C) > 260. μeff: 0 μB. Uv-Vis (DMF, λ_{max}, nm): 280, 331, 362, 383, 412, 434. Calculated for $C_{17}H_{20}Br_2N_2O_6Zn$ (%): C, 35.60; H, 3.51; N, 4.88. Found (%): C, 35.70; H, 3.69; N, 4.97.

$[Cd(HL)(H_2O)_2]\cdot 2H_2O$ (4), IR (ν, cm^{-1}): 3351, 2974, 1643, 1599, 1515, 1464, 1401, 1381, 1309, 1290, 1236, 1216, 1191, 1166, 1138, 1088, 1043, 968, 908, 870, 825, 795, 780, 672, 635, 619. Λ ($\Omega^{-1}\cdot cm^2\cdot mol^{-1}$) : 30 and 32 two weeks after. μeff: 0 μB. Uv-vis (DMF, λ_{max}, nm): 280, 331, 362, 383 π→π*, n→π*, TCLM. Yield: 80%, PF°C = 245. Calculated for $C_{17}H_{22}Br_2N_2O_7Cd$ (%): C, 33.91; H, 3.47; N, 4.39. Found (%): C, 33.89; H, 3.49; N, 4.45.

2.2.2.2 Complexes from metal nitrate salts

(0.2 g, 0.435 mmol) of H_3L was dissolved in 10 mL of absolute ethanol. A solution of $M(NO_3)_2\cdot xH_2O$ (M = Ni and Cu) (0.435 mmol) in 10 mL of absolute ethanol. The two solutions were mixed, and precipitate was instantly formed. The resulting suspension was then refluxed for two hours. After cooling, the solid was recovered and washed with 2 x 10 mL of ether and air-dried.

$[Ni(HL)(H_2O)_2]\cdot H_2O$ (5), IR (ν, cm^{-1}) : 3571, 2910, 1634, 1589, 1536, 1467, 1416, 1380, 1298, 1179, 1137, 1122, 1046, 997, 966, 875, 825, 800, 731, 705, 684, 639, 589, 474. μeff: 3.10 μB. Uv-vis (DMF, λ_{max}, nm): 371, 428, 447, 614. Λ ($\Omega^{-1}\cdot cm^2\cdot mol^{-1}$) : 119 and 112 two weeks after. Yield: 82%, PF°C > 260. Calculated for $C_{17}H_{20}Br_2N_2O_6Ni$ (%): C, 37.02; H, 3.56; N, 4.94, Found (%): C, 37.34; H, 3.43; N, 5.02.

$[Cu(HL)(H_2O)_2]\cdot H_2O$ (6), IR (ν, cm^{-1}): 3324, 2922, 1627, 1591, 1544, 1470, 1403, 1378, 1325, 1280, 1203, 1185, 1139, 1123, 1103, 1067, 1045, 976, 919, 876, 829, 818, 807, 794, 730. μeff: 1.81 μB. Uv-vis (DMF, λ_{max}, nm): 289, 390, 463, 633, 640 π→π*, n→π*, TCLM, d→d. Λ ($\Omega^{-1}\cdot cm^2\cdot mol^{-1}$): 40 and 41 two weeks after. Yield: 82%. MP(°C) > 250. Calculated for $C_{17}H_{20}Br_2N_2O_6Cu$ (%): C, 35.71; H, 3.53; N, 4.90. Found (%): C, 36.11; H, 3.57; N, 4.86.

2.3 X-ray Data Collection, Structure Determination and Refinement

Single crystals of $C_{17}H_{18}Br_2N_2O_5Ni$ (2) were grown by slow evaporation of MeOH solution of the complex. A suitable crystal was selected and mounted on a Bruker APEX-II CCD diffractometer with graphite monochromatized MoKα radiation (λ = 0.71073 Å). The crystal was kept at 173(2) K during data collection. Details of the X-ray crystal structure solution and refinement are given in Table 1. The structure was solved with the ShelXT [16] structure solution program using direct methods and refined with the ShelXTL [17] Software Package. All the structures were refined on F^2 by a full-matrix least-squares procedure using anisotropic displacement parameters for all non-hydrogen atoms. Molecular graphics were generated using *ORTEP-3* [18].

3. RESULTS AND DISCUSSION

3.1 General Studies

"The acyclic bicompartmental Schiff base H_3L have been prepared following a well-known method reported in the literature" [19-21]. "The synthesis of the ligand was achieved in a one-step procedure using the direct condensation of 1,3-diaminopropan-2-ol and 5-bromo-2-hydroxybenzaldehyde in molar ratio 1:1 with quantitative yield" [19-21] (Scheme 1). The infrared spectrum of the ligand shows a broad band at 3113 cm^{-1}, attributed to the ν_{O-H} vibration. The intense band at 1650 cm^{-1} is attributed to the $\nu_{C=N}$ vibration of the imine group formed during

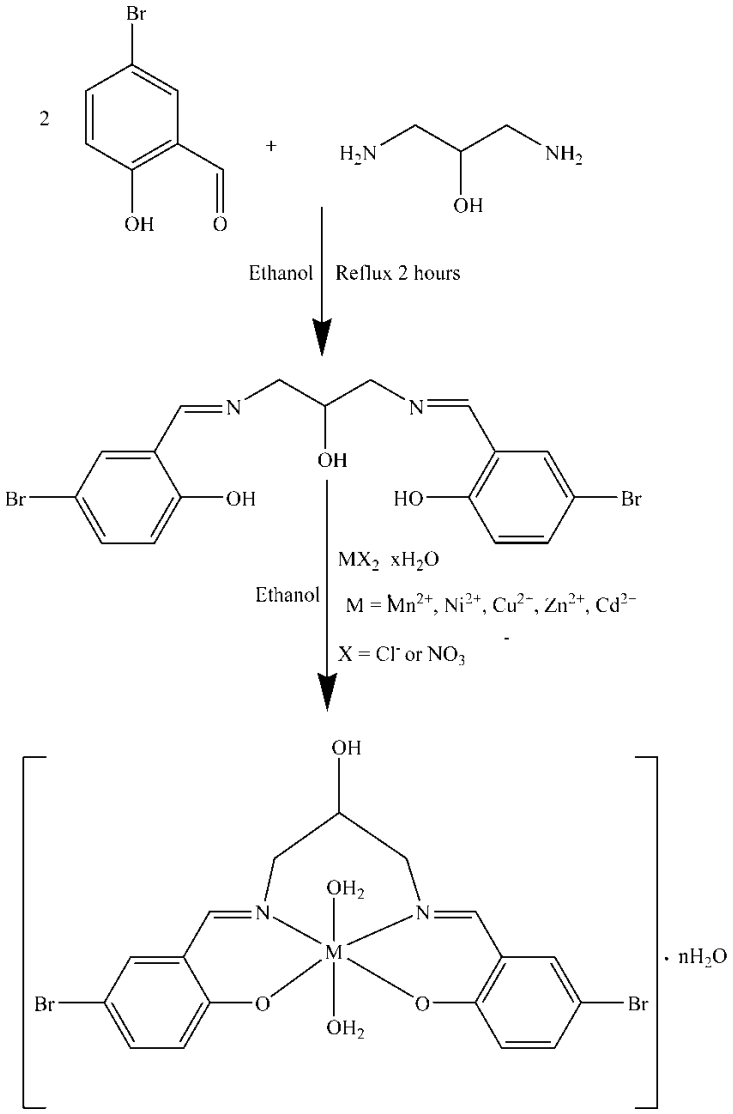

Scheme 1. General scheme for the synthesis of the ligand H_3L and its complexes

the condensation reaction between the aldehyde and the primary amine. The vibration band attributed to v_{Ar-O} is located at 1292 cm^{-1}. However, a valence vibration band pointed at 2803 cm^{-1} attributed to v_{Csp3-H}. The strong band around 1270 cm^{-1} is attributed to the v_{C-N} vibration. Nuclear magnetic resonance spectral of ^1H, ^{13}C and DEPT are recorded in DMSO. The ^1H NMR spectrum reveals two main singlet signals at 13.65 ppm and 8.51 ppm attributed to the phenolic and the azomethine protons, respectively. A signal as doublet pointed at 3.36 ppm is attributed to the methylene protons. A signal as multiplet at 3.65 ppm is attributed to the methinic proton. The alcoholic proton is pointed at 5.24 ppm. The aromatic protons are pointed in the range 8.80–7.67 ppm. The ^{13}C NMR spectrum reveals a signal at 165.84 ppm attributed to the azomethine carbon atoms. The signal at 160.49 ppm is attributed to phenolic carbon atoms. The signal at 69.02 ppm is attributed to carbon methinic carbon. The signals between 119.98 and 133.0 ppm are attributed to the carbon atoms of the aromatic ring. The DEPT spectrum shows that the signal appearing at 62.38 ppm is attributed to $–CH_2–$ carbon atoms. On the FTIR spectra of the complexes, the absorption band due to the azomethine function is shifted towards low frequencies compared to the v(C=N) band of the ligand which is, located at 1650 cm^{-1}. This band is pointed out in the spectra of the complexes at 1643 cm^{-1} and 1612 cm^{-1} for the Cd^{2+} and Mn^{2+} complexes, respectively. For the other complexes, this band is located in the range 1634 and 1592 cm^{-1}. A shift towards low frequencies is observed for the

v(C-O) phenolic bands, which point at 1274 cm^{-1} in the ligand FTIR spectrum. On the spectra of the complexes the above band appear in the range 1269 and 1251 cm^{-1}. These facts indicate that the nitrogen atom of the azomethine function and the phenolate oxygen atoms of the ligand are bonded to the metal ions. In the high frequency region of the spectra of the complexes, with the exception for copper complex valence vibration bands are observed around 3100 cm^{-1}. These bands are attributed to the v(OH) vibration of coordinated water molecules. The presence of coordinated water molecules is confirmed by the presence of the δ(OH) band at 869, 858 and 803 cm^{-1} for the cadmium, the nickel, and the zinc complexes, respectively. The absence of bands attributable to the vibrations of the nitrate ions suggest neutral complex. The infrared spectra of all complexes are very similar, suggesting similar structures. Measurements of the molar conductivity of the complexes are carried out using a molar solution of DMF. The conductimetric measurements of the complexes are presented in Table 2. The values obtained with fresh solutions are consistent with neutral electrolytes for complexes (1)–(4) and (6). After two weeks of storage, the values indicate that the complexes are still neutral electrolytes. For complexes obtained from nitrate salts, the conductivity varies from one complex to another. The slight variation of the values is indicative of high stability of the complexes in DMF. The complex (5) which is a 1:2 electrolyte is probably unstable in DMF solution. The UV–vis spectra of the complexes show π → π* and n → π* transition bands in the [280–289] and [331–390] nm regions, respectively. A ligand metal charge transfer (LMCT) band is observed around 428 nm for the complex of nickel (II). Four d → d transition bands are also identified in the electronic spectrum of the Ni(II),complex at 666, 633, 606 and 579 nm. The UV-visible spectrophotometric data for the complexes are listed in Table 2. The study of the UV-visible spectrophotometry of the different complexes indicates that for complex (1), in addition to the transition bands π→π* and n→π*due to chromophores groups such as C=N, there are ligand-metal charge transfer (LMCT) bands between 430 and 515 nm. The bands at 576 nm and 583 nm are probably due to the electronic transition $^6A_1 \rightarrow {}^4T_{2g}$ and $^6A_1 \rightarrow {}^4T_{1g}$, respectively. These facts are in agreement with an octahedral geometry around the Mn(II) ion [21,3,22]. Two of the three bands expected for octahedral Ni(II) complex are pointed at 428 and 606 nm in the spectrum of the complex (2) of Ni(II). The absence of the third transition band is probably due to its low intensity. These two values are attributed, respectively, to the transitions $^3A_{2g} \rightarrow {}^3T_{2g}(P)$ and $^3A_{2g} \rightarrow {}^3T_{1g}(F)$, indicating an octahedral environment around Ni(II)[3]. Complexes (3) and (4) exhibit similar bands at 280, 331, 362 and 383 nm. These bands can be assigned to the transition bands in the chromophore groups of the organic ligand. In addition to the transition bands π→π* and n→π*, the spectrum of complex (3) which has a metallic center d^{10} presents two absorption bands at 412 and 434 nm. These bands are assigned to the metal-ligand charge transfer (TCML). The spectrum of complex (5) shows four bands pointed at 371, 428, 447 and 614 nm, which are due to ligand-metal charge transfer and $^3A_{2g} \rightarrow {}^3T_{2g}(P)$ and $^3A_{2g} \rightarrow {}^3T_{1g}(F)$ transitions, indicating an octahedral environment of a Ni(II) complex [23,24]. On the spectrum of the Cu(II) complex (6), the bands at 463, 633, and 640 nm are both assigned to the d→d transition. The width of the bands at 666 and 640 nm indicates the presence of an hexacoordinated environment around copper(II) ions [25].

Constant-temperature magnetic susceptibility data for the synthesized complexes are given in Table 2. The Zn(II) (3) and Cd(II) (4) complexes are diamagnetic [26,27], i.e. they have zero magnetic moment. The manganese (II) and nickel (II) complexes have magnetic moments of 5.54 and 2.68 μB respectively [26]. These values are slightly lower than those for free Mn(II) and Ni(II) ions respectively. The Ni(II) complex shows this pseudo-octahedral character because of the low value of 2.68 μB [28]. For complex (5), the value of the magnetic moment is 3.10 μB. This value corresponds to two unpaired electrons for a Ni(II) ion with an ideal six-coordination configuration. The Cu(II) complex (6) has a magnetic moment equal to 1.81 μB, corresponds to a Cu(II) with a single electron and describes an octahedral environment around the Cu(II) ion [29,30].

The cadmium complex (4) in DMSO, excited at 372 nm, fluoresces at 465 nm. Excited with a wavelength of 372 nm, the cadmium complex (4), at a concentration of 266.6 μg/mL in DMSO, emits intra-ligand fluorescence (π→π*) at 465 nm. When the concentration increases from 133.3 μg/mL to 266.6 μg/mL, a significant increase in fluorescence is observed with a positive deviation of λ_{em}. From 266.6 μg/mL to 400 μg/mL, a slight increase in fluorescence

intensity is observed (Fig. 1) without any shift in λ_{em}. Fluorescence intensity is concentration dependent only in the range [0 –133.3 μg/mL]. An increase in concentration results in saturation of the medium, and the solvent DMSO, which is also a ligand, can coordinate with Cd(II) ions. The direct consequence of this strong electro donation is an increase in fluorescence.

3.2 Structure description of the complex $[Ni(HL)(H_2O)_2]$ (2)

Complex (2) crystallizes in the centrosymmetric orthorhombic system with the space group *Pmna*. The selected bond distances and angles are shown in Table 3. The asymmetric unit contains a mononuclear complex consisting of a di-deprotonated ligand molecule, a nickel(II) ion, and two coordinated water molecules. The *ORTEP* diagram of the structure of the nickel complex is shown in Fig. 2. The coordination of the ligand to the nickel metal occurs via two phenolate oxygen atoms, two azomethine nitrogen atoms and two water molecules oxygen atoms, thus giving a mononuclear entity in which, the Ni(II) ion is located in an N_2O_4 environment. The environment around the metal ion is best described as a square-based octahedron. The basal plane is occupied by the oxygen and nitrogen atoms of the ligand while the axial positrons are occupied by the oxygen atoms of the coordinated water molecules. The *cissoid* bond angles are in the range 84.77 (7)–98.74 (7)°, while the *transoid* angles are 172.81 (5)° and 172.81 (5)°. The sum of the angles subtended by the atoms in the basal plane is 359.95°. The atoms in the basal plane and the Ni(II) form an almost perfect plane (rms 0.001) with the Ni(II) slightly out-of-plane by 0.024 Å. The angle defined by the atoms in axial position [O1W—Ni1—O2W] is 170.7 (7)°. These values indicate a slight deformation of the octahedron. The base plane bond lengths [Ni1—O1 = 2.0303 (11) Å and Ni1—N1 = 2.0492 (12) Å] are shorter than the axial bond lengths [Ni1—O1W = 2.0955 (19) Å and Ni1—O2W = 2.1071 (18) Å].

Table 1. Crystallographic data and refinement parameters for $C_{17}H_{18}Br_2N_2O_5Ni$

Chemical formula	$C_{17}H_{18}Br_2N_2O_5Ni$
Shape and color	Prism, green
Molar Mass g/mol	548.84
Crystal system	Orthorhombic
Crystal size (mm)	0.400 x 0.300 x 0.200
Temperature	100 K
Wavelength Mo *K*α radiation,	0.71073 Å
Space group	*Pnma*
a (Å)	7.7702(4)
b (Å)	23.1921(7)
c (Å)	10.6853(5)
$\alpha = \beta = \gamma$ (°)	90
Volume Å^3	1925.57(15)
Z	8
D_{calc} g/cm^3	1.893
F(000)	1088
μ (mm^{-1})	5.19
θ(°)	2.2-30.1
H, k, l ranges	-15 ≤ h ≤15, -21≤ k ≤20, -46 ≤ l ≤ 46
Measured reflections	52291
Independent reflections	8099
Reflections [I>= 2σ(I)]	5216
R_{int}	0.065
Independent reflections	8099
R [I>2σ(I)]	0.043
wR_2	0.121
Goodness-of-Fit	1.07
Data / restraints / parameters	8099 / 0 / 139
$\Delta\rho_{max}$, $\Delta\rho_{min}$ (e Å^{-3})	3.36 / -2.66

Table 2. Electronic data, magnetic moments, and complex conductance data

Compound	UV Bands		Λ ($\Omega^{-1}cm^2mol^{-1}$)		μ/μB
	π → π*, n→ π*, MLCT	d→d	Fresh	two weeks after	
$H_3L = C_{17}H_{20}Br_2N_2O_3$	265, 280, 331, 362				
$[Mn(HL)(H_2O)_2]\cdot H_2O$ (**1**)	395, 412, 430, 472, 515, 576	583	23	26	5.54
$[Ni(HL)(H_2O)_2]$(**2**)	282, 371, 428	606	27	33	2.68
$[Zn(HL)(H_2O)_2]\cdot H_2O$ (**3**)	280, 331, 362, 383, 412, 434		25	28	Diam
$[Cd(HL)(H_2O)_2]\cdot 2H_2O$ (**4**)	280, 331, 383		30	32	Diam
$[Ni(HL)(H_2O)_2]\cdot H_2O$ (**5**)	371, 428, 447	614	119	112	3.10
$[Cu(HL)(H_2O)_2]\cdot H_2O$ (**6**)	289, 385, 463, 633	639	40	41	1.81

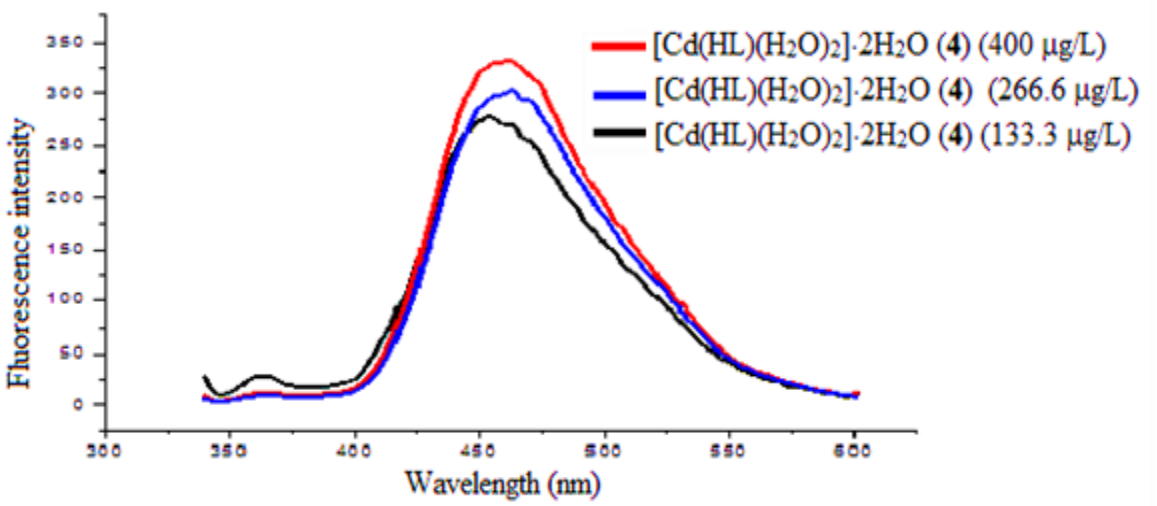

Fig. 1. Emission spectra of the complex $[Cd(HL)(H_2O)_2]\cdot 2H_2O$ (4) in DMSO excited at 372 nm at different concentrations.

The ligand coordination defines two six-membered NiOCCCN rings and one six-membered NiNCCCN ring with bite angles of 88.22(5)° and 98.74(7)°, respectively. The two NiOCCCN cycles form intersecting planes with a dihedral angle of 25.06° and each of them forms with the NiNCCCN plane a dihedral angle of 12.74°. Intermolecular hydrogen bond involving the water molecule oxygen atom of the coordinated water molecule and phenolate oxygen atom of the ligand [O2w—H2w···O1^{iv}, iv = *x*−1/2, −*y*+3/2, −*z*+3/2 and O1w—H1w···O1^{v}, v = *x*+1/2, −*y*+3/2, −*z*+3/2] are observed. In the crystal, unclassical intermolecular C—H···Br [C7—H7···Br^{i}, i = −x+1/2, −y+1, z−1/2; C8A—H8A··· Br^{ii}, ii = −x+1, −y+1, −z+1] and C—H···O [C8B—H8B···O2A^{iii}, iii = x+1/2, y, −z+1/2] interactions are also observed in the crystal (Table 4, Fig. 2).

3.3 Antibacterial activity of the H_3L ligand and its complexes {$[Cd(HL)(H_2O)_2]\cdot 2H_2O$} (4) and {$[Ni(HL)(H_2O)_2]\cdot H_2O$} (5)

For this triad of compounds, the diameters of the inhibition zones are between 16 and 35 mm for the H_3L ligand and the complex (4) reflecting greater antibacterial activity [31-33] than for complex (5) which shows relatively low activity. For the activity on *Escherichia coli*, the diameters of the inhibition zone of the H_3L ligand and its cadmium complex (4) are, respectively, 18 and 28 mm for a concentration of 30 mg/mL. The activities of the ligand and the complex (4) on *Salmonella. SP*, are practically identical to those on *Escherichia coli*. For *Pasteurella multocida*, the complex (4) has very good activity against this strain, with an inhibition diameter of

35 mm. With respect to this last strain, the H_3L ligand shows average activity with an inhibition diameter equal to 16 mm for a concentration of 30 mg/mL. Complex (5) presents inhibition diameters equal to 6 mm on all strains at a concentration of 30 mg/mL. This complex can be declared inactive. The minimum inhibitory concentration (MIC) values obtained tell us about the effectiveness of the compounds [34]. The H_3L ligand is active against *Escherichia coli*, *Salmonella sp* and *Pasteurella multocida* from a MIC of 0.06 mg/mL while at this same concentration, complex (4) is active against the *Salmonella sp* and *Pasteurella multocida* strains. Complex (4) is active against *Escherichia coli* with a MIC of 0.12 mg/mL. The results of testing the biological activity of the studied ligand and complexes are given in diagram 1. Most metal chelates show higher antimicrobial activity against microorganisms than those of free ligands.

Table 3. Selected interatomic bond distances and bond angles around Ni

Ni1—O2W	**2.1071 (18)**	**Ni1—O1W**	**2.0955 (19)**
Ni1—O1	2.0303 (11)	Ni1—N1	2.0492 (12)
Ni1—O1^{i}	2.0303 (11)	Ni1—N1^{i}	2.0493 (12)
O1—Ni1—O2W	93.46 (5)	O1—Ni1—N1^{i}	172.81 (5)
O1^{i}—Ni1—O2W	93.47 (5)	O1^{i}—Ni1—N1^{i}	88.22 (5)
O1—Ni1—O1^{i}	84.77 (7)	O1W—Ni1—O2W	170.34 (7)
O1^{i}—Ni1—O1W	93.67 (6)	N1—Ni1—O2W	85.35 (5)
O1—Ni1—O1W	93.67 (6)	N1^{i}—Ni1—O2W	85.35 (5)
O1—Ni1—N1	88.22 (5)	N1^{i}—Ni1—N1	98.74 (7)
O1^{i}—Ni1—N1	172.81 (5)		

Symmetry code: (i) x, −y+3/2, z.

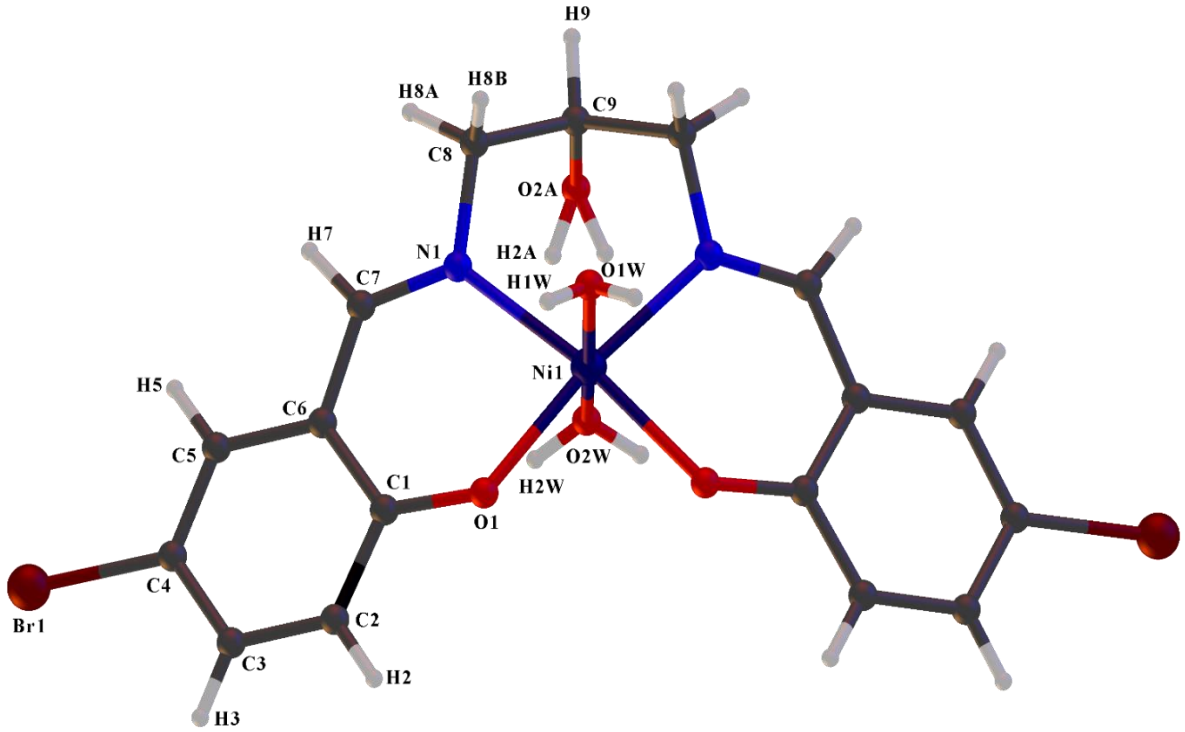

Fig. 2. ORTEP plot (30% probability ellipsoids) showing the structure of 2.

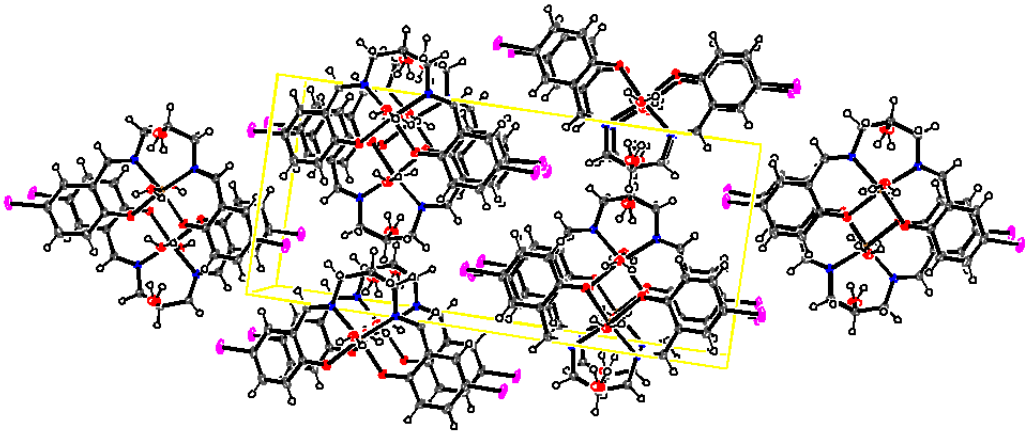

Fig. 3. The packing of the compound in the crystal structure

Table 4. Hydrogen-bond geometry (Å, °)

D—H···*A*	D—H	H···*A*	*D*···*A*	*D*—H···*A*
C7—H7···Br1^{i}	0.95	3.06	3.8825(15)	145.3
C8—H8A···Br1^{ii}	0.99	3.12	3.7979(15)	126.9
C8—H8B···O2A^{iii}	0.99	2.52	3.149(3)	121.1
O2W—H2W···O1^{iv}	0.80(3)	1.91(3)	2.6258(19)	148(3)
O1W—H1W···O1^{v}	0.73(3)	2.15(4)	2.836(2)	156(4)

Symmetry codes: (i) −x+1/2, −y+1, z−1/2; (ii) −x+1, −y+1, −z+1; (iii) x+1/2, y, −z+1/2; (iv) x−1/2, −y+3/2, −z+3/2; (v) x+1/2, −y+3/2, −z+3/2.

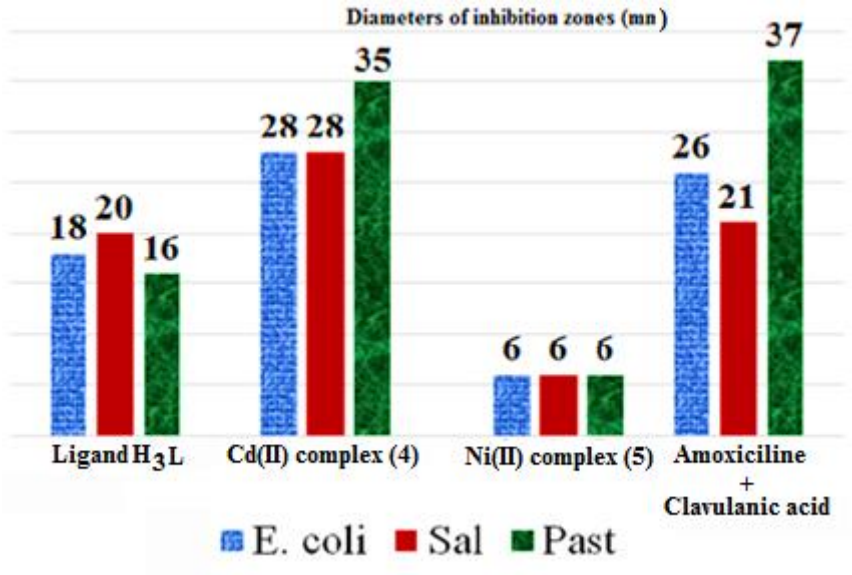

Diagram 1. Antibacterial tests of the H_3L ligand and complexes (4), (5)

The diagram below shows that the ligand is more effective than the nickel(II) complex while the Cd(II) complex has a higher efficiency than the H_3L ligand. The increase in activity of complex (4) relative to the H_3L ligand is probably due to the presence of cadmium(II) ion while the drop in activity for the complex (5) suggests that nickel(II) plays a role as an inhibitor of antibacterial activity. Complex (4) is more active than the antibiotic reference on *Escherichia coli* and *Salmonella sp* and its activity on *Pasteurella multocida* is almost equal to the activity of the reference.

4. CONCLUSION

The synthesis and characterization of the Schiff base ligand 2,2'-[(2-hydroxypropane-1,3-diyl) bis-(imino-methanediyl)]bis-(4-bromophenol), six metal transition complexes were synthesized and were studied using spectroscopic and spectrophotometric methods as well as X-ray diffraction technique for nickel(II) complex (2). The dianionic ligand acts in tetradentate mode via two azomethine nitrogen atoms and two oxygen phenolate atoms. Infrared spectroscopy confirms the coordination between the Schiff base ligand and the cations Mn(II), Ni(II), Cu(II), Zn(II) and Cd(II). The structure of complex (2) is determined by single crystal x-ray diffraction. The environment around each cation is octahedral. The cadmium complex (4) in DMSO, is excited at a wavelength of 372 nm with a concentration of 133.3 μg/mL, it emits fluorescence at 465 nm which is attributed to an intra-ligand transition π-π*).The increase in emission wavelength is a function of concentration in the range [0 -133.3] μg/mL. Beyond this range, any increase in concentration leads to an increase in fluorescence without affecting λ_{em}, until saturation is reached. Antibacterial tests on three known strains have shown that the non-deprotonated organic ligand and the cadmium(II) complex (4) have better activity than the nickel(II) complex (5). The activity of the organic ligand is closer to that of the reference, which is amoxicillin and clavulanic acid.

SUPPLEMENTARY MATERIALS

CCDC-2310883 contains the supplementary crystallographic data for this paper. These data can be obtained free of charge via https://www.ccdc.cam.ac.uk/ structures/, or by contacting The Cambridge Crystallographic Data Centre, 12 Union Road, Cambridge CB2 1EZ, UK.

COMPETING INTERESTS

Authors have declared that no competing interests exist.

REFERENCES

1. Dongli C, Handong J, Hongyun Z, Deji C, Jina Y, Jian LB. Studies on acetylferrocenyl nicotinoyl and isonicotinoyl hydrazones and their coordination compounds with transition metals—ii. Polyhedron. 1994;13(1):57–62. Available:https://doi.org/10.1016/S0277-5387(00)86638-3
2. Gueye A, Tamboura FB, Planeix JM, Gruber N, Gaye M. Synthesis and spectroscopic study of transition metal complexes of tridentate ligand formed by direct condensation of o-vanillin and 2-aminophenol: X-Ray Structural Characterization of the Zinc(II) Complex. Eur. J. Chem. 2018;9(4):281–286. Available:https://doi.org/10.5155/eurjchem.9.4.281-286.1761
3. Kane CH, Tinguiano D, Tamboura BF, Thiam IE, Barry AH, Gaye M, Retailleau P. Synthesis and characterization of novel M(II) (M = Mn(II), Ni(II), Cu(II) or Zn(II)) complexes with tridentate N2,O-Donor Ligand (E)-2-Amino-N'-[1-(Pyridin-2-Yl)-Ethylidene]benzohydrazide. Bull. Chem. Soc. Ethiop. 2016;30(1): 101. Available:https://doi.org/10.4314/bcse.v30i1.9
4. Yang H, Liu SS, Meng YS, Zhang YQ, Pu L, Yu XQ. Magnetic properties and theoretical calculations of mononuclear lanthanide complexes with a schiff base coordinated to ln(iii) ion in a monodentate coordination mode. Inorg. Chim. Acta 2019;494:8–12. Available:https://doi.org/10.1016/j.ica.2019.04.051
5. Neverov A, McDonald T, Gibson G, Brown R. Catalysis of transesterification reactions by lanthanides - unprecedented acceleration of Methanolysis of Aryl and Alkyl Esters Promoted by La(OTf)3 at Neutral s spH and ambient temperatures. Can. J. Chem. 2001;79:1704–1710. Available:https://doi.org/10.1139/cjc-79-11-1704
6. Van Vleck, J H, Frank A. The effect of second order zeeman terms on magnetic susceptibilities: Errata. Phys. Rev. 1929; 34(12):1625–1625. Available:https://doi.org/10.1103/PhysRev.34.1625
7. Mohamad, ADM, Abualreish MJA, Abu-Dief AM. Antimicrobial and anticancer activities of cobalt (iii)-hydrazone complexes: Solubilities and chemical potentials of transfer in different organic co-solvent-water mixtures. J. Mol. Liq. 2019;290:111162. Available:https://doi.org/10.1016/j.molliq.2019.111162.
8. Eldehna W, Fares M, Abdel-Aziz M, Abdel-Aziz, Design H. Synthesis and

antitubercular activity of certain nicotinic acid hydrazides. Molecules. 2015;20(5): 8800–8815.
Available:https://doi.org/10.3390/molecules20058800

9. Hussain M, Shafiq Z, Hussain A, Yaqub M, Arshad S, Ashraf M, Abbasi BH, Ahmad HB. Synthesis and antioxidant and antibacterial activities of metal-based schiff bases of nicotinoyl, isonicotinoyl and benzoyl hydrazides. Asian J. Chem. 2013; 25(5):2593–2596.
Available:https://doi.org/10.14233/ajchem.2013.13495
10. Shen S, Chen H, Zhu T, Ma X, Xu J, Zhu W, Chen R, Xie J, Ma T, Jia L, Wang Y, Peng C. Synthesis, Characterization and anticancer activities of transition metal complexes with a nicotinohydrazone ligand. Oncol. Lett. 2017;13(5):3169–3176.
Available:https://doi.org/10.3892/ol.2017.5857
11. Ramalakshmi N, Aruloly L, Arunkumar S, Ilango K, Puratchikody A. Synthesis and biological evaluation of some novel nicotinic acid derivatives. Malays. J. Sci. 2009;28(2):197–203.
Available:https://doi.org/10.22452/mjs.vol28no2.8
12. Singh YP, Patel RN, Singh Y, Butcher RJ, Vishakarma PK, Singh RKB. Structure and antioxidant superoxide dismutase activity of copper(ii) hydrazone complexes. Polyhedron. 2017;122:1-15.
Available:https://doi.org/10.1016/j.poly.2016.11.013
13. Londoño-Mosquera JD, Aragón-Muriel A, Polo Cerón D. Synthesis, Antibacterial activity and dna interactions of lanthanide(iii) complexes of N(4)-substituted thiosemicarbazones. Univ. Sci. 2018;23(2):141169.
Available:https://doi.org/10.11144/Javeriana.SC23-2.saaa
14. Bakale RP, Naik GN, Machakanur SS, Mangannavar CV, Muchchandi IS, Gudasi KB. Structural characterization and antimicrobial activities of transition metal complexes of a hydrazone ligand. J. Mol. Struct. 2018;1154:92–99.
Available:https://doi.org/10.1016/j.molstruc.2017.10.035
15. Hartwig A, Asmuss M, Blessing H, Hoffmann S, Jahnke G, Khandelwal S, Pelzer A, Bürkle A. Interference by toxic metal ions with zinc-dependent proteins involved in maintaining genomic stability. food chem. Toxicol. 2002;40(8):1179–1184.
Available:https://doi.org/10.1016/S0278-6915(02)00043-1
16. Sheldrick GM. SHELXT – Integrated Space-Group and Crystal-Structure Determination. Acta Crystallogr. Sect. Found. Adv. 2015;71(1):3–8.
Available:https://doi.org/10.1107/S2053273314026370
17. Sheldrick GM. Crystal structure refinement with SHELXL. Acta Crystallogr. Sect. C Struct. Chem. 2015;71(1):3–8.
Available:https://doi.org/10.1107/S2053229614024218
18. Farrugia LJ. WinGX and ORTEP for windows : An Update. J. Appl. Crystallogr. 2012;45(4):849–854.
Available:https://doi.org/10.1107/S0021889812029111
19. Gueye A, Tamboura FB, Sy A, Gaye M, Gruber N, Jouaiti A. Six new transition metal mononuclear complexes Of N'-(5-bromo-2-hydroxybenzylidene) nicotinohydrazide Schiff Base. Synthesis, Spectroscopic Characterization And X-ray structure Determination of the Zinc (II) Complex. IOSR J. Appl. Chem. 2019; 12(4):24-30.
Available:https://doi.org/10.9790/5736-1204012430
20. Fellah FZC, Boulefred S, Fellah AC, El Rez B, Duhayon C, Sutter JP. Binuclear CuLn complexes (Ln^{III}= Gd, Tb, Dy) of alcohol-functionalized bicompartmental Schiff-base ligand. Hydrogen bonding and magnetic behaviors. Inorg. Chim. Acta. 2016;439:24-29.
Available:https://doi.org/10.1016/j.ica.2015.09.032
21. Kulkarni NV, Sathisha MP, Budagumpi S, Kurdekar GS, Revankar VK. Binuclear transition metal complexes of bicompartmental SNO donor ligands: Synthesis, Characterization, and Electrochemistry. J. Coord. Chem. 2010; 63(8):1451–1461.
Available:https://doi.org/10.1080/00958971003770405
22. Xu S, Smith JET, Weber JM. UV Spectra of Tris(2,2′-Bipyridine)–M(II) Complex Ions in Vacuo (M = Mn, Fe, Co, Ni, Cu, Zn). Inorg. Chem. 2016;55(22):11937–11943.
Available:https://doi.org/10.1021/acs.inorgchem.6b02054
23. Chakraborty P, Majumder I, Sabnam Banu K, Ghosh B, Kara H, Zangrando E, Das D.

Mn(Ii) complexes of different nuclearity: Synthesis, Characterization and catecholase-like activity. Dalton Trans. 2016;45(2):742–752.
Available:https://doi.org/10.1039/C5DT03659C

24. Despaigne AAR, Silva JGD, Carmo ACM do, Piro OE, Castellano EE, Beraldo H. Structural studies on zinc(ii) complexes with 2-benzoylpyridine-derived hydrazones. Inorg. Chim. Acta. 2009; 362(7):2117–2122.
Available:https://doi.org/10.1016/j.ica.2008.09.040.
25. Cao S, Cheng R, Wang D, Zhao Y, Tang R, Yang X, Chen J. Dinuclear copper (II) complexes of “end-off” bicompartmental ligands: Alteration of the chelating arms on ligands to regulate the reactivity of the complexes towards DNA. J. Inorg. Biochem. 2019;192:126-139.
Available:https://doi.org/10.1016/j.jinorgbio.2018.12.014
26. Refat MS, Altalhi T, Bakare SB, Al-Hazmi GH, Alam K. New Cr (III), Mn (II), Fe (III), Co (II), Ni (II), Zn (II), Cd (II), and Hg (II) gibberellate complexes: synthesis, structure, and inhibitory activity against COVID-19 protease. Russ. J. Gen. Chem. 2021;91(5):890-896.
Available:https://doi.org/10.1134/S1070363221050194
27. Ali MA. Magnetic and spectroscopic studies on nickel (II) and copper (II) complexes of some neutral tridentate ONS ligands. Can. J. Chem. 1980;58(7):727-732.
Available:https://doi.org/10.1139/v80-112
28. Shanmuga Bharathi K, Sreedaran S, Anitha Ayswarya R, Kalilur Rahiman A, Rajesh K, Narayanan V. Synthesis, Spectral, Magnetic, Electrochemical, and kinetic studies of copper (II), nickel (II) and zinc (II) complexes derived from a phenol-based unsymmetrical “end-off” ligand. J. Coord. Chem. 2009;62(4):600-612.
Available:https://doi.org/10.1080/00958970802302246
29. El-Behery M, El-Twigry H. Synthesis, Magnetic, Spectral, and antimicrobial studies of Cu(II), Ni(II) Co(II), Fe(III), and UO_2(II) complexes of a new Schiff base hydrazone derived from 7-chloro-4-hydrazinoquinoline. Spectrochim. Acta A Mol. Biomol. Spectrosc. 2007;66(1):28-36.
Available:https://doi.org/10.1016/j.saa.2006.02.017
30. Iliopoulos P, Fallon GD, Murray KS. Structural, Spectroscopic, and magnetic properties of mono-and bi-nuclear copper (II) complexes of N-(2-pyridinyl) ketoacetamides. J. Chem. Soc. Dalton Trans. 1986;437-443.
Available:https://doi.org/10.1039/DT9860000437
31. Dakanali M, Kefalas ET, Raptopoulou C P, Terzis A, Mavromoustakos T, Salifoglou A. Synthesis and spectroscopic and structural studies of a new cadmium (ii)− citrate aqueous complex. potential relevance to cadmium (ii)−citrate speciation and links to cadmium toxicity. Inorg. chem. 2003;42(8):2531-2537.
Available:https://doi.org/10.1021/ic0205029
32. Xie Q, Liu N, Lin D, Qu R, Zhou Q, Ge F. The complexation with proteins in extracellular polymeric substances alleviates the toxicity of Cd (II) to Chlorella vulgaris. Environ. Pollut. 2020;263:114102.
Available:https://doi.org/10.1016/j.envpol.2020.114102
33. El-Sherif AA, Eldebss TM. Synthesis, spectral characterization, solution equilibria, in vitro antibacterial and cytotoxic activities of Cu (II), Ni (II), Mn (II), Co (II) and Zn (II) complexes with Schiff base derived from 5-bromosalicylaldehyde and 2-aminomethylthiophene. Spectrochim. Acta A Mol. Biomol. vSpectrosc. 2011;79(5):1803-1814.
Available:https://doi.org/10.1016/j.saa.2011.05.062
34. Gikas P. Single and combined effects of Nickel (Ni(II)) and Cobalt (Co(II)) Ions on Activated Sludge and on Other Aerobic Microorganisms: A Review. J. Hazard. Mater. 2008;159(2):187–203.
Available:https://doi.org/10.1016/j.jhazmat.2008.02.048

SUPPLEMENTARY MATERIALS

The NMR Spectra of the organic ligand successively (1H-NMR, 13C-NMR and DEPT-135)

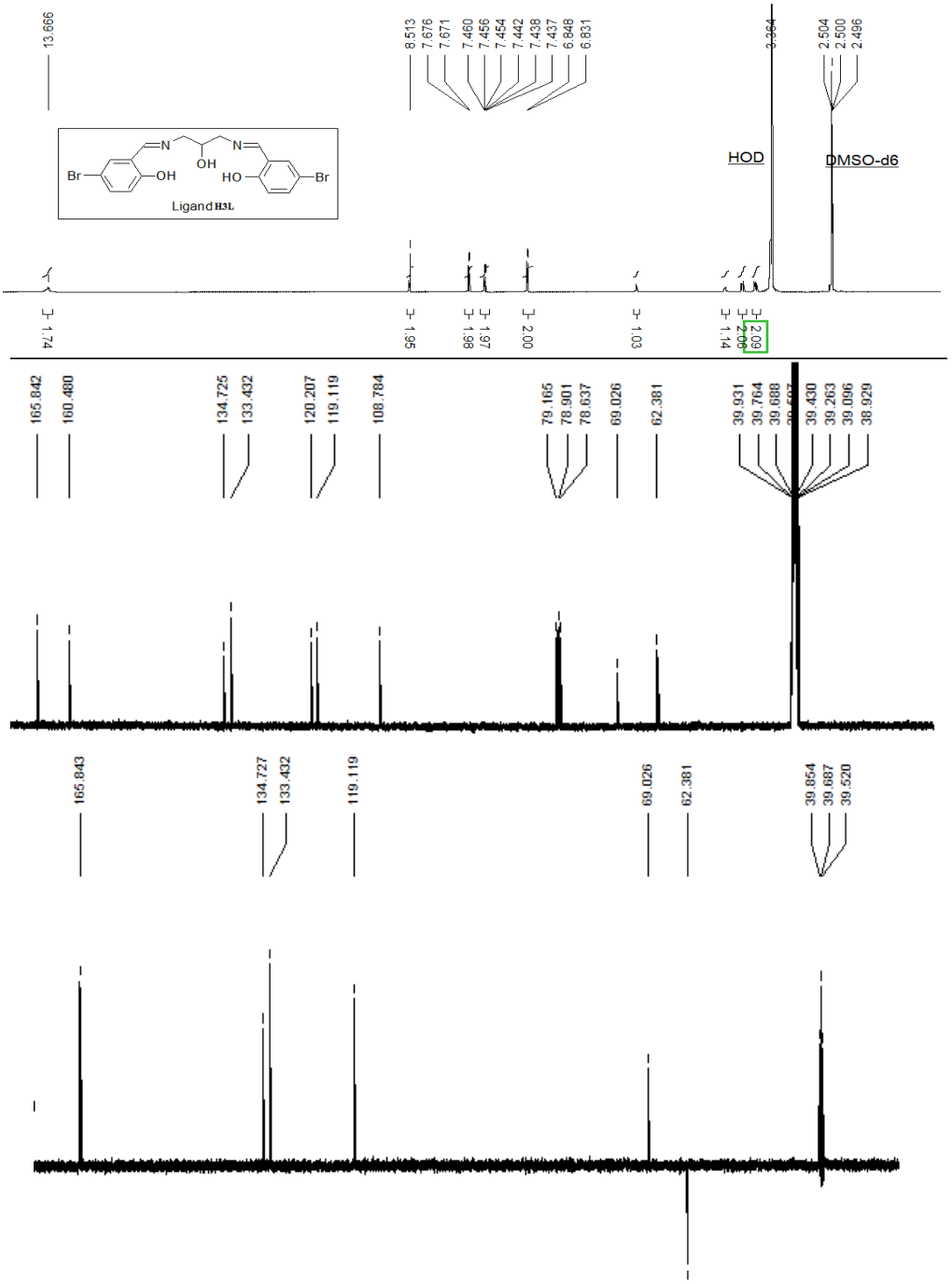

Peer-review history:
The peer review history for this paper can be accessed here:
https://www.sdiarticle5.com/review-history/111342